Remote End-to-End Dosimetry Auditing Service Report

@ Hospital

Report reviewed by: Evangelos Pappas,
Associate Professor of Medical Physics,
University of West Attica

Audit outcome: 

Date: DDth Month YYYY

RTsafe
48, Artotinis str
116 33, Athens
Greece
+30 2107563691
info@rt-safe.com

Institution:	Hospital
Date of audit:	Month DD YYYY
Date of report:	Month DD YYYY
Institution's contact person:	Name
	Professor of Medical Physics
Responsible for OSLD results:	Name
Responsible for Film dosimetry results:	Name
Report prepared by:	Kyveli Zourari
Report reviewed by:	Evangelos Pappas
Phantom:	Prime
Treatment planning system:	TPS
Treatment delivery modality:	LINAC / CK / GK
Treatment delivery unit:	Model
Image Guidance/setup/positioning protocol:	CBCT
Audit Reference Number:	NNYYSUCADV
Phantom S/N:	0121PRM
Film Insert Kit S/N:	3620FDK
OSLD Insert Kit S/N:	0220OSLDK
Gel Insert Kit S/N (empty-gel / filled):	NNYYGDKE / NNYYGDKE

Contents

Introduction

RTsafe's succeS^{R}S is a remote end-to-end dosimetry audit service for intracranial stereotactic radiosurgery applications (SRS). The primary objective of succeS^{R}S is to evaluate the dosimetric quality, planned dose accuracy and treatment deliverability of brain SRS procedures for the improvement of standards and reliability of the institutions.

The scope of this report is to:

- Present and assess the dosimetric impact of all steps of the SRS treatment pathway through an end-to-end test, i.e., immobilization, pre-treatment imaging, treatment planning, setup - image guidance and dose delivery, and
- Outline the quality of the delivered treatment in the radiotherapy center based on point, 2D and 3D dosimetry results, as recorded and reviewed from the dosimetry audit.

The phantom used in the audit was the RTsafe Prime phantom, using the specially designed inserts to accommodate Gafchromic EBT film, optically stimulated luminescent (OSL) and polymer gel dosimeters (Figure 1). All the dosimeters are calibrated at the Secondary Standard Dosimetry Laboratory of the Greek Atomic Energy Commission, providing traceability to BIPM-France. The users received a multi-target RT structure set, and were challenged to achieve a specific level of accuracy for the required treatment objectives.

Figure 1: The RTsafe Prime phantom used in the audit, along with the specially designed inserts to accommodate Gafchromic EBT film, OSL and polymer gel dosimeters.

Audit Procedures

Preparation for the audit

@ Hospital received the Prime phantom (RTsafe P.C.) on Month DDth YYYY. Prime was accompanied with the corresponding inserts for film, OSL and gel dosimeters. For absolute point OSL dosimetry, the corresponding insert was pre-loaded with 17 calibrated OSLDs (Figure 2a), allowing measurements in the coronal plane. Similarly, for absolute 2D dosimetry, one (1) calibrated pre-cut EBT-3 film was available (Figure 2b). For relative 3D gel dosimetry, a water-filled cylinder was included in the package for imaging and planning purposes (Figure 2c). The gel-filled cylinder was delivered to the institution the scheduled day of irradiation, i.e., Month DDth YYYY.

The phantom was prepared for CT scanning using all the necessary immobilization devices, as per department protocol, for a single-isocenter multiple-metastasis stereotactic radiosurgery treatment. Then three consecutive CT scans were performed, one for each detector, with the film and OSL detectors in place. The 3rd CT scan was performed with the water-filled cylinder in place, to create the required CT dataset for the 3D dosimetry planning purposes.

A separate/reference dataset of the benchmark case (CT scan of the phantom with the targets and organs at risk (OAR) volumes) was provided in DICOM format via the RTsafe secure sharing platform. All CT scans were imported into the Treatment Planning System (TPS). All targets were delineated such that their center of mass lies at the film plane. There were three spherically-shaped targets located centrally in the brain. Two of them were located along the underside of the brain near the brainstem.

All CT scans of the phantom were co-registered in the TPS. The delineated contours were propagated to the local CT scans onto which the dose calculations were performed. Figure 2 shows a schematic of the location of the OSL and film dosimetry cassettes, as well as the gel cylindrical insert, relative to the PTV and OARs.

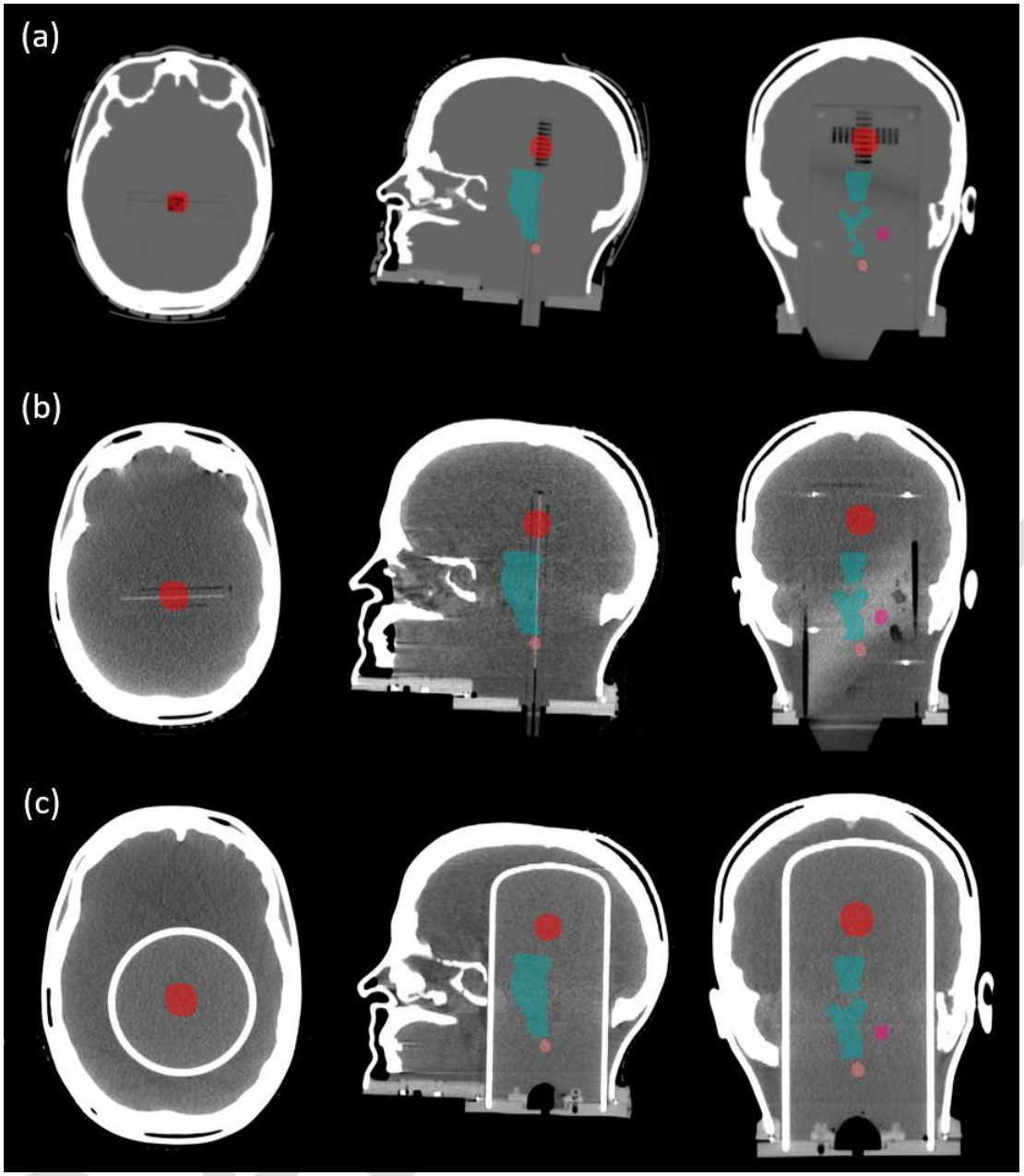

Figure 2: Schematic representation of the axial, sagittal and coronal planes through the phantom showing (a) all OSL, (b) film and (c) polymer gel dosimeters.

The SRS treatment plan was generated following the local protocol by the staff members who normally perform the patient treatment planning and exported to the treatment delivery platform. The treatment objectives that the user was asked to achieve during the planning process are shown in Table 1. A VMAT treatment plan was generated using Eclipse. The DICOM RT plan, dose, and structure set files were sent back to RTsafe via the RTsafe secure sharing platform.

Table 1: Treatment optimization objectives & dose goals.

Structure:		
PTVs	80% of volume to receive at least 2400 cGy	3 fractions
Quality metrics:		
CI RTOG or Paddick[a]	> 0.7	
GI Paddick[b]	PTV 1: < 3 PTV 2: < 5 PTV 3: < 5	
Q[c]	> 0.9	

[a] $CI_{RTOG} = \frac{V_{RI}}{\mathrm{TV}}$, RTOG conformity index or $CI_{Paddick} = \frac{TV^2_{PIV}}{\mathrm{TV} \times \mathrm{PIV}}$, Paddick conformity index

[b] $GI_{Paddick} = \frac{PIV_{half}}{PIV}$, Paddick gradient index

[c] $Q = \frac{I_{min}}{RI}$, Quality of coverage

where, TV : target volume
PIV : prescription isodose volume
TV_{PIV} : target volume covered by the prescription isodose
I_{min} : minimun dose given to the target
RI : prescriprion isodose
PIV_{half} : volume covered by the 50% of prescription dose

SRS plan delivery

The end-to-end procedure was performed by the RT center staff according to the local protocol.

Three different dosimetry inserts were used; the OSL dosimetry cassette, the film dosimetry cassette, and the gel-filled cylindrical insert. Thus, the institution subsequently irradiated three times (3) the Prime phantom.

Plan data was sent to the TrueBeam EDGE linear accelerator for delivery. The Prime phantom incorporating the OSLD cassette was treated first and was localized with a CBCT scan, which was fused with the planning CT data set. 6D corrections were applied prior to delivery. The process was repeated for the film and gel measurements.

After completion, the Prime phantom and the three dosimetry inserts were returned to RTsafe. The OSL and film dosimeters were unloaded for analysis, and the Prime phantom incorporating the irradiated gel-filled cylinder was MR scanned for the dose read-out at the RTsafe reference MR scanner 24 hours post irradiation.

The end-to-end dosimetric and geometric accuracy were evaluated. Absolute (OSLDs & films) as well as relative dose distributions (polymer gel) agreement with TPS calculations was assessed in terms of 1D dose profiles and 1D gamma index, 2D isolines and 2D gamma index maps and 3D gamma index passing rates for each target. The geometrical offset of the planned and polymer gel-measured dose distributions was also assessed.

Auditors assessments

SRS plan evaluation

The submitted treatment plan parameters are shown in Table 6.

Table 6: Treatment plan parameters.

Treatment plan name:	FILM 1fr/ GEL-film/ OSL-film
Technique:	HyperArc
Treatment delivery modality:	LINAC
Treatment delivery unit:	TrueBeam EDGE
TPS:	Eclipse 15.6 – HyperArc
Energy (MV):	6
Total monitor units (MUs):	2156.6
Dose prescription:	24 Gy @ 80%
Number of fractions:	3
Dose per fraction (Gy):	8
Dose grid resolution (x, y, z):	1 mm x 1 mm x 1 mm
CI RTOG:	PTV 1: 0.78
	PTV 2: 0.57
	PTV 3: 0.63
GI Paddick:	PTV 1: 5.21
	PTV 2: 14.23
	PTV 3: 15.09
Q:	PTV 1: --
	PTV 2: --
	PTV 3: --
CT scan in plane resolution (mm):	0.78 x 0.78
CT scan slice thickness (mm):	1
MR scan in plane resolution (mm):	1.37
MR scan slice thickness (mm):	2

OSL dosimetry

Point-dose comparison

Table 7 shows the OSLD results for each dosimeter. Results from dosimeters lying at high dose gradient regions were excluded from the analysis. An energy correction factor was applied to the OSLD results to take into account the decrease in sensitivity of the dosimeters when calibrated in ^{60}Co energy and irradiated at higher energies.

To facilitate the reader to understand the results, the following Figure 3 shows the position of the dosimeters on the cassette.

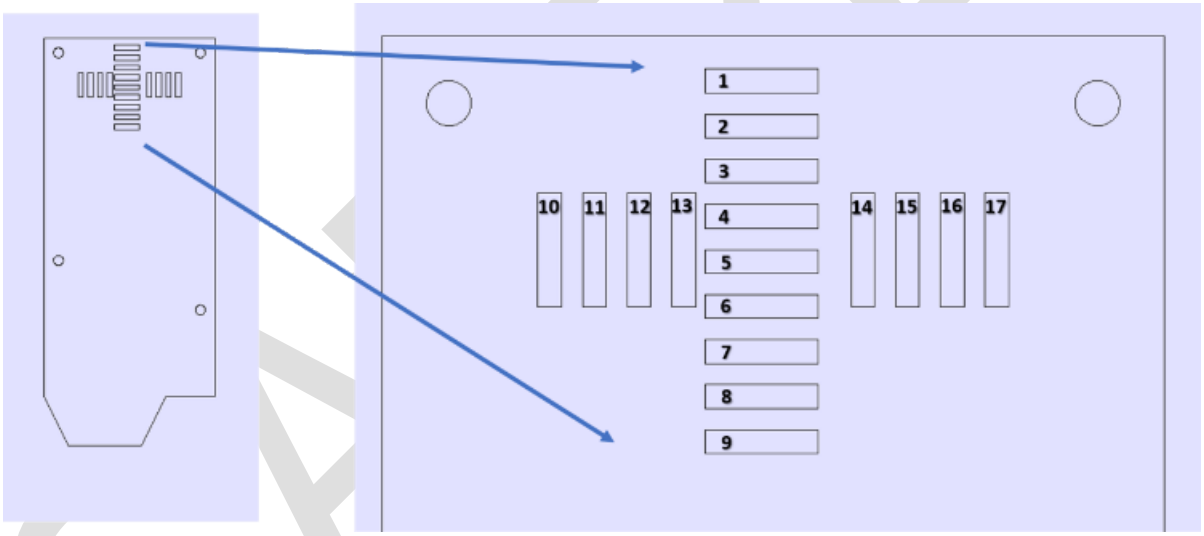

Figure 3: Schematic representation of the dosimetry cassette placed along the coronal plane through the phantom showing all OSL dosimeters.

Table 7: OSL dosimetry results during the end-to-end procedures using Prime phantom. The total combined uncertainty at k=1 is ± 4%.

a/a	OSL dosimeter S/N	TPS calculated dose (Gy)	OSL measured dose (Gy)	Dose difference (%)
4	DC09302816J	7.92	7.64	3.66
5	DC09215893D	7.84	7.82	0.26
6	DC09112718H	7.98	7.70	3.64
7	DN08970096O	7.94	8.15	-2.58
13	DC09215836D	7.66	7.96	-3.77
14	DC09010900X	7.91	7.60	4.08

Profile's comparison

Lateral (right-left) and superior-inferior absolute dose profiles for the OSL-measured and TPS-calculated datasets for PTV 1 are presented in the following figures 4 & 5, respectively. 4% error bars are also shown for the OSL measurements.

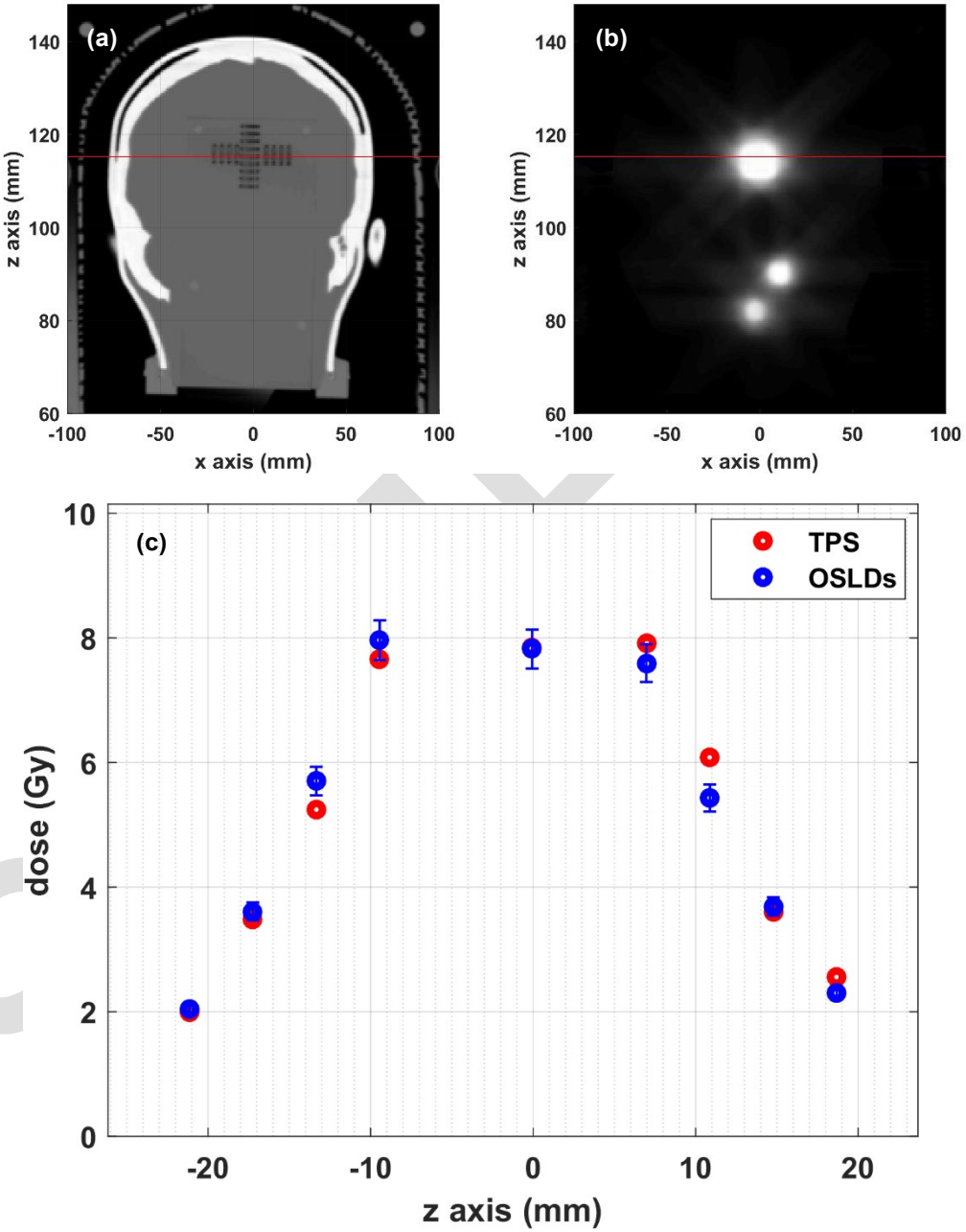

Figure 4: Lateral dose profile for PTV 1 - (a) Slice of the reconstructed CT scan of the OSLDs phantom and (b) Slice of the exported RTDOSE calculated on the OSLDs phantom. The red solid line displays the direction in which the OSLDs effective volumes lie. (c) 1D profile comparison between calculated (TPS) and measured (OSL) dose measurements at the dosimeters locations depicted by the red line.

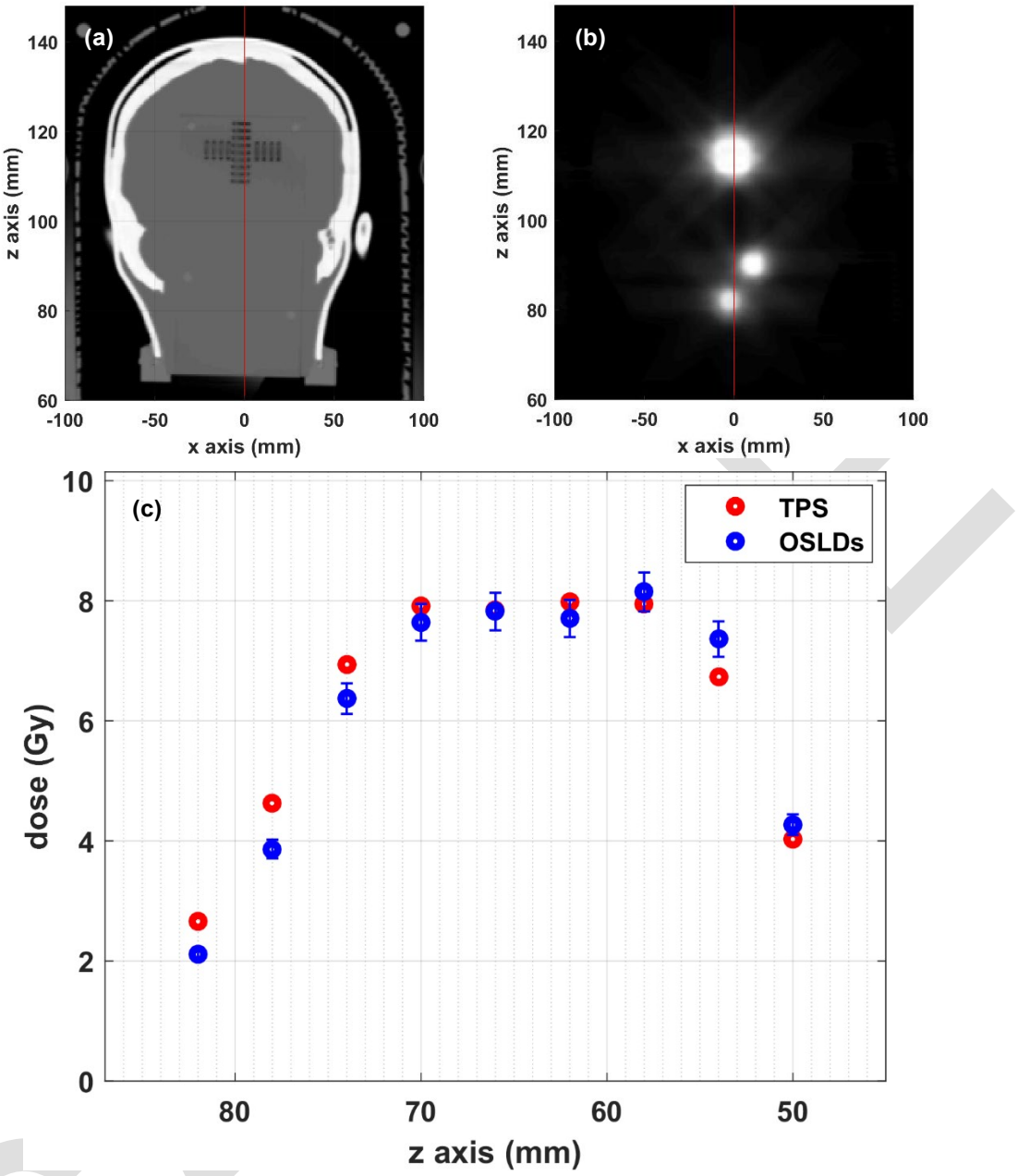

Figure 5: Superioinferior dose profile for PTV 1 - (a) Slice of the reconstructed CT scan of the OSLDs phantom and (b) Slice of the exported RTDOSE calculated on the OSLDs phantom. The red solid line displays the direction in which the OSLDs effective volumes lie. (c) 1D profile comparison between calculated (TPS) and measured (OSL) dose measurements at the dosimeters locations depicted by the red line.

Film dosimetry

Profile's comparison

A right-left and a superior-inferior absolute dose profiles for the film-measured and TPS-calculated datasets are presented in the following figures 6-11 for all targets.

R-L – Coronal orientation

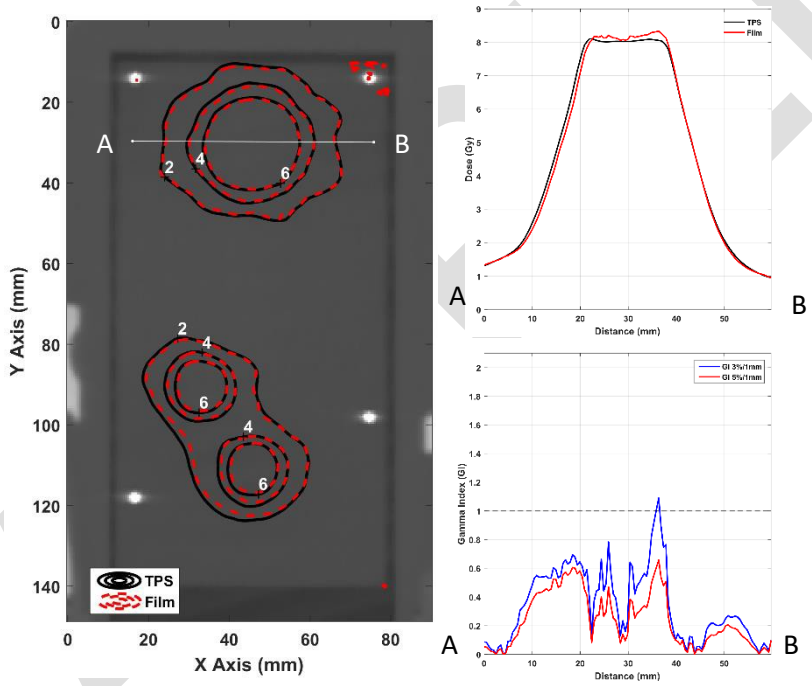

Figure 6: PTV 1 - (left) Slice of the reconstructed CT scan of the film phantom. Contours correspond to TPS calculations (black solid lines) and film measurements (red dashed lines) in Gy. (right) 1D profile comparison between calculated (TPS) and measured (Film) dose distributions at the location depicted by the white line. 1D gamma index calculations are also given using passing criteria 3%/1mm & 5%/1mm.

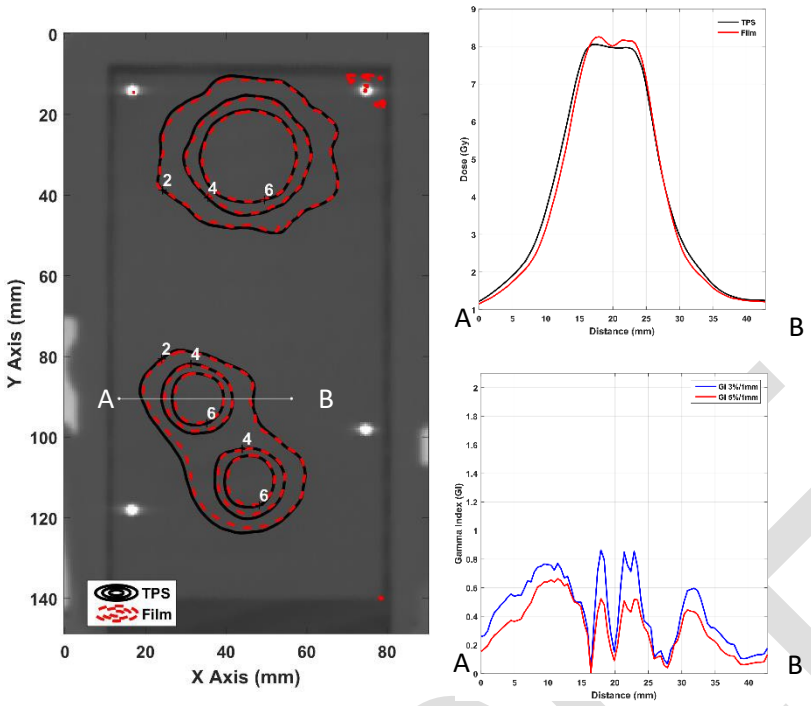

Figure 7: PTV 2 - (left) Slice of the reconstructed CT scan of the film phantom. Contours correspond to TPS calculations (black solid lines) and film measurements (red dashed lines) in Gy. (right) 1D profile comparison between calculated (TPS) and measured (Film) dose distributions at the location depicted by the white line. 1D gamma index calculations are also given using passing criteria 3%/1mm & 5%/1mm.

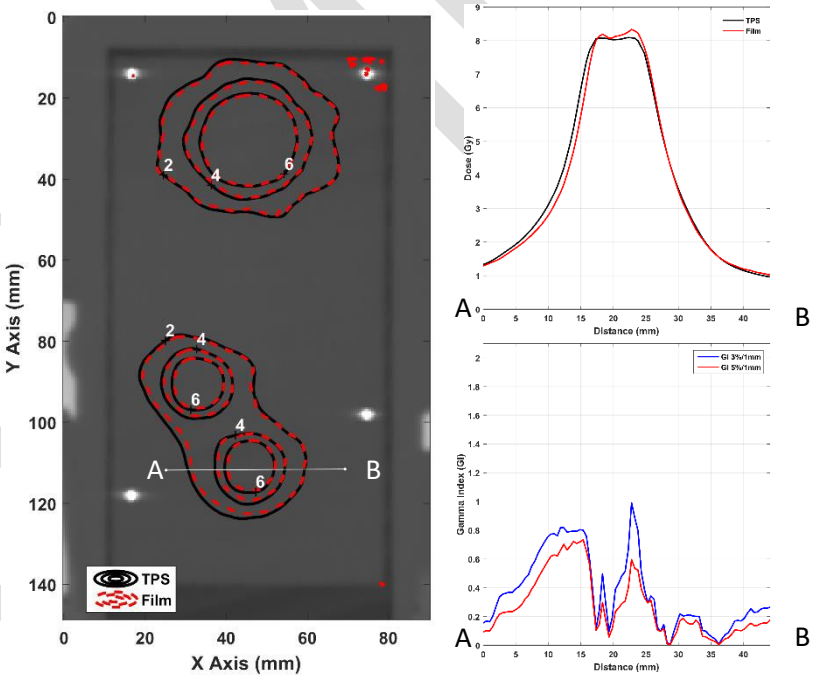

Figure 8: PTV 3 - (left) Slice of the reconstructed CT scan of the film phantom. Contours correspond to TPS calculations (black solid lines) and film measurements (red dashed lines) in Gy. (right) 1D profile comparison between calculated (TPS) and measured (Film) dose distributions at the location depicted by the white line. 1D gamma index calculations are also given using passing criteria 3%/1mm & 5%/1mm.

Sup-Inf – Coronal orientation

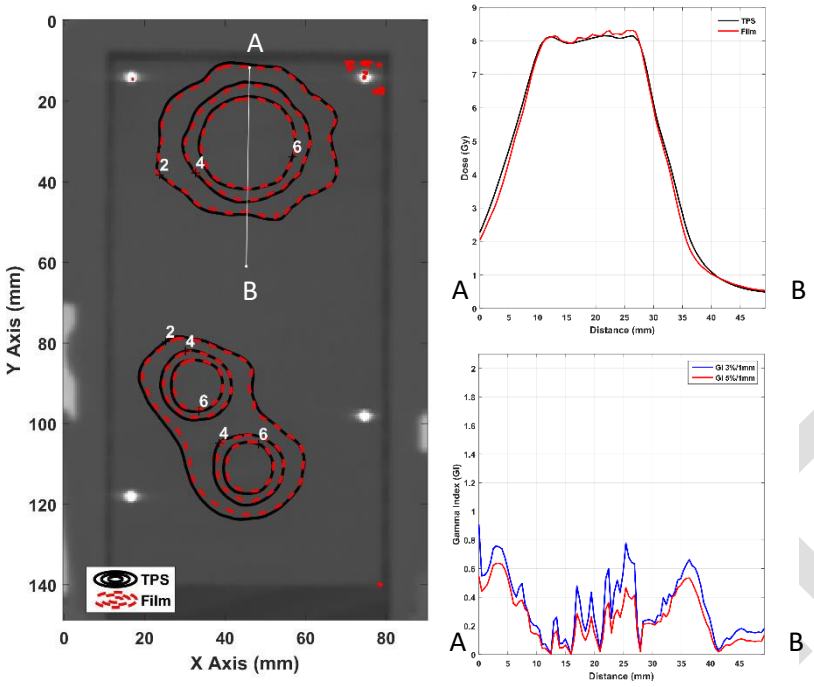

Figure 9: PTV 1 - (left) Slice of the reconstructed CT scan of the film phantom. Contours correspond to TPS calculations (black solid lines) and film measurements (red dashed lines) in Gy. (right) 1D profile comparison between calculated (TPS) and measured (Film) dose distributions at the location depicted by the white line. 1D gamma index calculations are also given using passing criteria 3%/1mm & 5%/1mm.

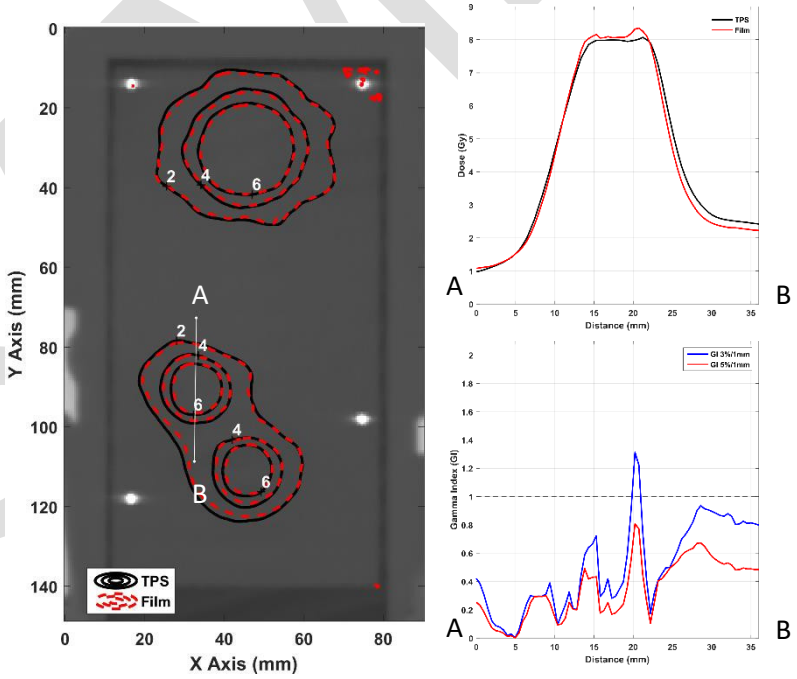

Figure 10: PTV 2 - (left) Slice of the reconstructed CT scan of the film phantom. Contours correspond to TPS calculations (black solid lines) and film measurements (red dashed lines) in Gy. (right) 1D profile comparison between calculated (TPS) and measured (Film) dose distributions at the location depicted by the white line. 1D gamma index calculations are also given using passing criteria 3%/1mm & 5%/1mm.

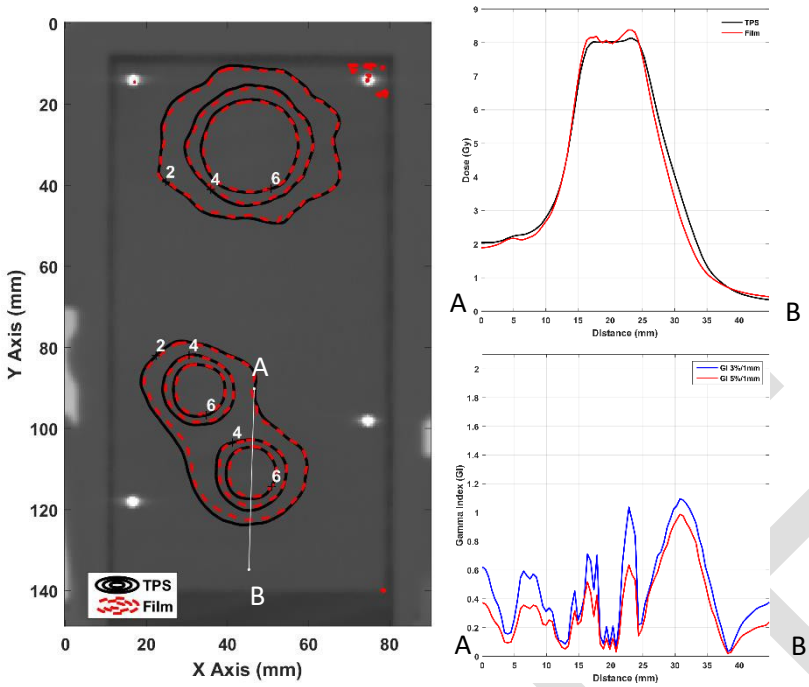

Figure 11: PTV 3 - (left) Slice of the reconstructed CT scan of the film phantom. Contours correspond to TPS calculations (black solid lines) and film measurements (red dashed lines) in Gy. (right) 1D profile comparison between calculated (TPS) and measured (Film) dose distributions at the location depicted by the white line. 1D gamma index calculations are also given using passing criteria 3%/1mm & 5%/1mm.

2D Gamma Index comparison

For the slice between film cassette slabs of the film phantom, 3D gamma index calculations (i.e., reference data: 2D film measurements, evaluated data: 3D TPS calculations) are presented in the following figures. Passing criteria were 3%/1mm and 5%/1mm dose difference and distance-to-agreement, respectively. A low-dose cut-off threshold of 10% of the prescription dose has been applied to exclude corresponding voxels from the gamma index calculations. Isodose lines are also plotted to assist comparison.

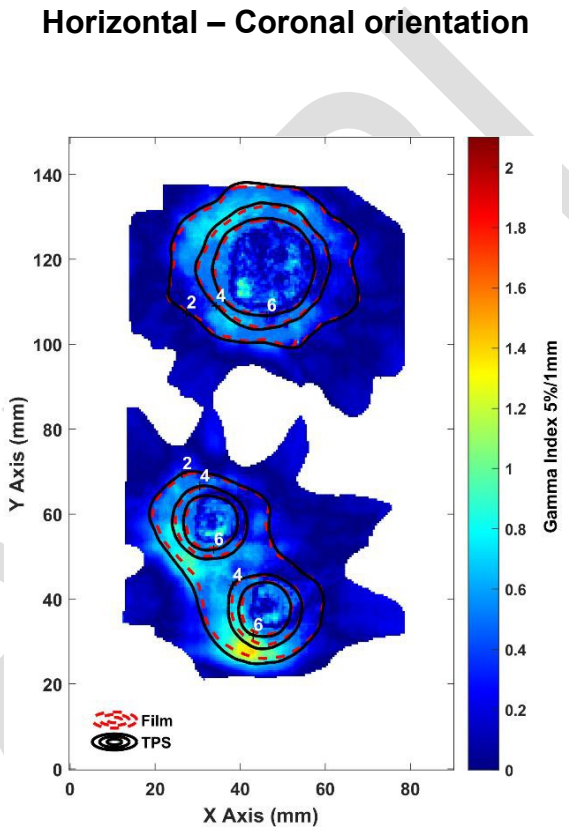

Figure 12: 2D comparison between calculated (TPS) and measured (Film) dose distributions in Gy values applying a 10% low-dose cut-off threshold. 3D gamma index calculations are given using passing criteria 5%/1mm.

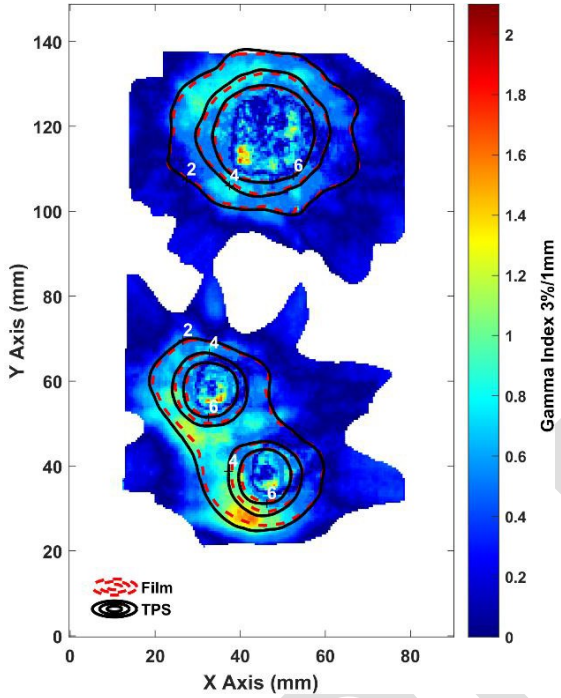

Figure 13: 2D comparison between calculated (TPS) and measured (Film) dose distributions in Gy values applying a 10% low-dose cut-off threshold. 3D gamma index calculations are given using passing criteria 3%/1mm.

3D Gamma Index comparison

Gamma index calculations were also performed in 3D. A selection of gamma passing rates suitable for SRS plan analysis were chosen. The gamma passing rates presented were collected using the red color channel covering the area of the film, with a low-dose cut-off threshold for doses below 80 cGy (10% of the prescription dose). Corresponding results are summarized in the following table 8.

Table 8: Results for the 3D gamma index test of Film 1 in coronal orientation (Horizontal), comparing film-measured (reference) with the TPS-calculated (evaluated) dose distributions using a variety of passing criteria. Note that passing rates were calculated using a low-dose cut-off threshold of 10% of the prescribed dose.

Structure	Passing criteria		Global GI Passing Rate
	DD (%)	DTA (mm)	GI ≤ 1 (%)
Film Plane	3	3	99.62
	3	2	99.55
	3	1	96.93
	2	2	98.72
	5	**1**	**99.17**

To quantify the overall performance and adequacy of the dosimetric commissioning, the tolerance limits, proposed by AAPM-RSS Medical Physics Practice Guideline 9.a. for SRS-SBRT were adopted. In detail, using SRS frame and/or IGRT system, the E2E localization assessment should be ≤ 1.0 mm and the E2E dosimetric evaluation should lie within ± 5% difference of the measured versus the calculated dose distributions. Therefore, for the gamma analyses, the tolerance limit is set to ≥ 95%, with 5%/1 mm and a 10% low-dose cut-off threshold and the action limit to ≥ 90%, with 5%/1 mm and a 10% low-dose cut-off threshold, having a gamma <1.

Gel dosimetry

Qualitative comparison

Image registration between post-irradiation MRI and planning RTDose TPS data with structures of the Prime phantom. This is to demonstrate the coincidence of each treated target to its planned location.

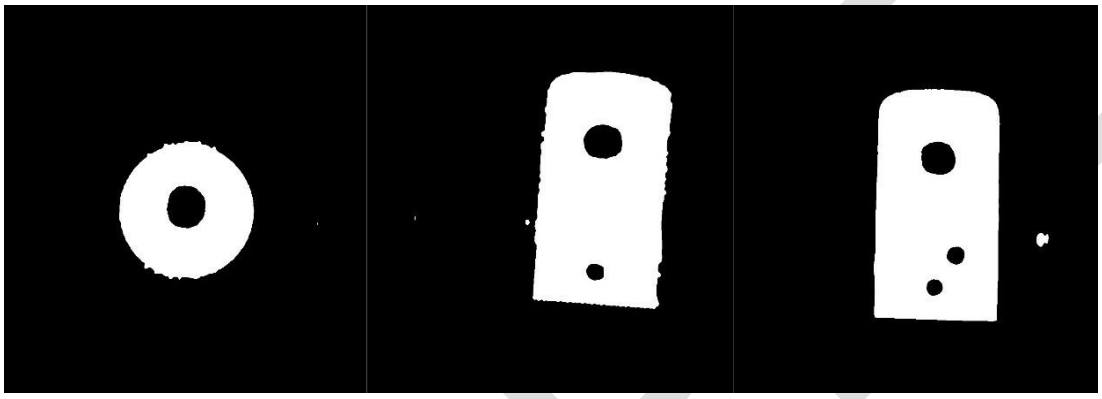

Gel relative dose 100% - RTDOSE TPS 0%

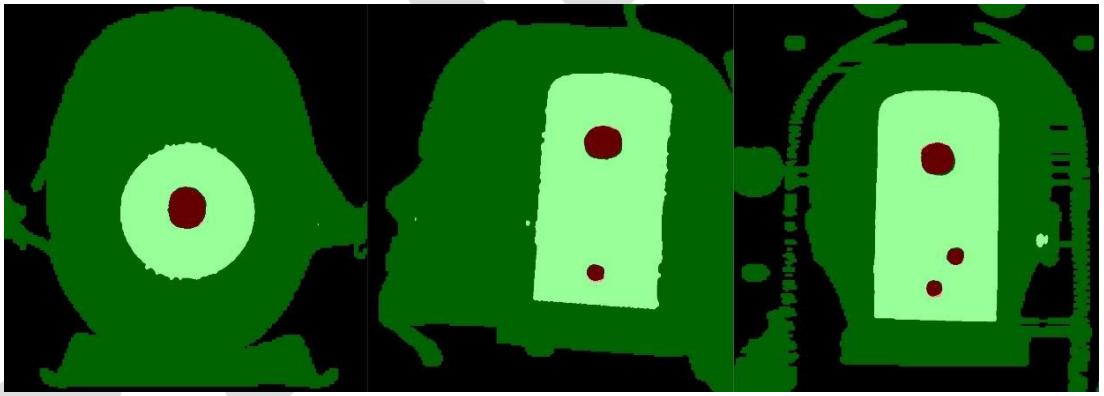

Gel relative dose 50% - RTDOSE TPS 50%

Gel relative dose 0% - RTDOSE TPS 100%

Figure 11: Illustration of the relative dose map depicted from the MRI scans of the gel blended with TPS DICOM RT data. Brightness and contrast are adjusted so that high dose areas are depicted.

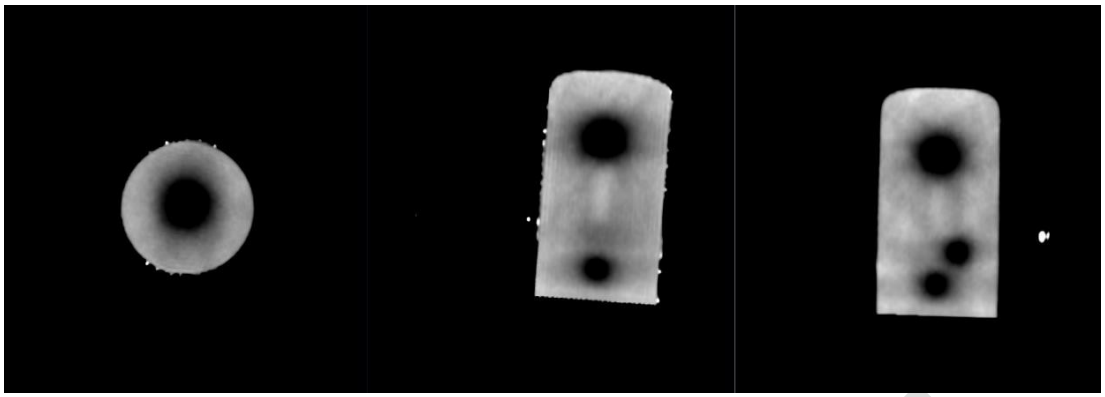

Gel relative dose 100% - RTDOSE TPS 0%

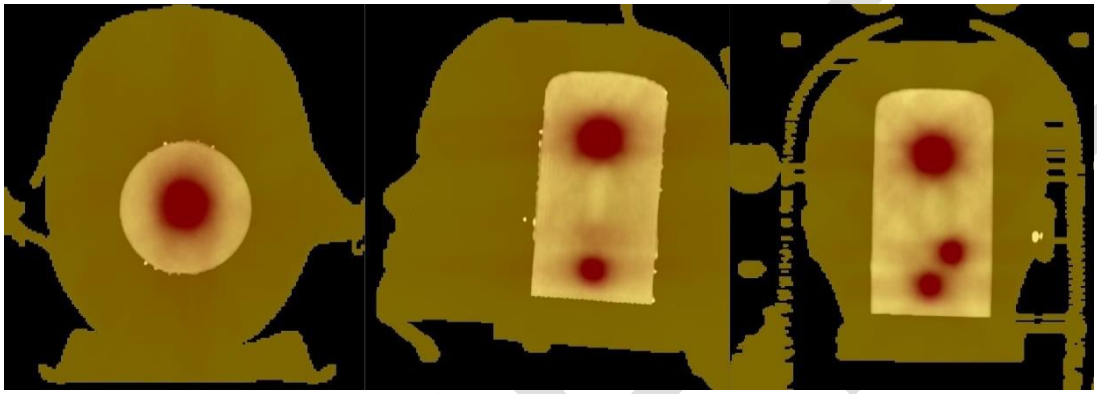

Gel relative dose 50% - RTDOSE TPS 50%

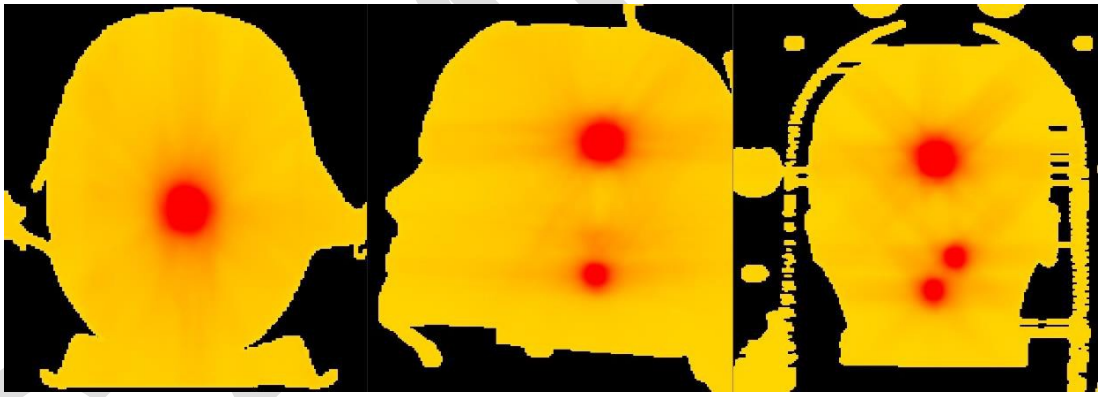

Gel relative dose 0% - RTDOSE TPS 100%

Figure 12: Illustration of the MRI (actually delivered dose) blended with TPS (calculated dose). Brightness and contrast are adjusted so that low dose areas are depicted.

Geometry offset evaluation

Figure 13 shows the distribution of the calculated center of mass (CoM) coordinates for each direction. To assess the total spatial offset of the planned dose distribution and the corresponding gel-measured dose distribution for each target, the geometric distance between the center of masses was calculated (APPENDIX). Results are summarized in Table 9 separately for the x, y, z coordinates, i.e., Right-Left, Anterior-Posterior and Superior-Inferior directions respectively, as well as for the total spatial offset. The distance between the CoM of each target and the plan isocenter is also given.

Table 9: Results of the calculated distances between (a) the CoM coordinates of each target and the planning isocenter and (b) the x CoM coordinates i.e., R-L direction, (c) the y CoM coordinates i.e., A-P direction, (d) the z CoM coordinates i.e., S-I direction, and (e) the total spatial offset, of the polymerized area and the planned high-dose area for the structures considered.

	(a) Target distance from ISO (mm)	(b) x - axis offset (mm)	(c) y - axis offset (mm)	(d) z - axis offset (mm)	(e) Total geometric offset (mm)
PTV 1	46.902	0.073 ± 0.029	0.115 ± 0.050	0.761 ± 0.088	0.773 ± 0.008
PTV 2	16.488	0.244 ± 0.032	0.330 ± 0.043	0.186 ± 0.041	0.450 ± 0.002
PTV 3	33.559	0.034 ± 0.036	0.184 ± 0.061	0.784 ± 0.051	0.806 ± 0.003

Comparison to national and international intracranial SRS audit results

--

Audit outcome

Our analysis performed has not indicated any concerns regarding the local practices for the specific aspects of dosimetry for intracranial stereotactic radiosurgery. All dose computations during treatment planning (calculation algorithm, medium corrections, dose reporting) are in compliance with RTOG protocol requirements. As it was beyond the objectives of this study, critical organ dose-volume data are not presented, however, organ-at-risk doses were constrained in accordance with RTOG protocol guidelines. OSLDs response within steep dose gradients is associated with high level of uncertainty and therefore it should be used for information only. Dosimetry results meet the listed acceptance criteria proposed by AAPM AAPM-RSS Medical Physics Practice Guideline 9.a. for SRS-SBRT.

Disclaimer

The results recorded in this report were deduced based on procedures performed by the end-user following the guidelines of RTsafe staff. Results are presented "as is". No warranties, express or implied, that these results are free of error is made. This action serves as an external evaluation of dosimetry and radiation protection practices of the institution and is supplementary to the internal evaluations, measurements, and quality control tests of its routine quality assurance program. These results should in no case be used as the institution's reference values. Reference values are determined by the local physics team, based on the full program of commissioning of the institution. The presented dosimetric report should not be relied on for solving a problem whose incorrect solution could result in injury to a person or loss of property. RTsafe shall not, in any event, be liable for any damages, whether direct or indirect, special or general, consequential or incidental, arising from the use of the results of this report. RTsafe does not suggest any specific actions for improving your radiotherapy treatment protocol. The responsibility for the accuracy of clinical treatment delivery remains with the local center.

APPENDIX. Dosimeter's readout and analysis process

OSL dosimetry

The phantom incorporating the OSLD dosimetry case is similar to the detailed description in the publication of Makris et al 2019[1]. The difference is that instead of the film cassette, the OSLD cassette of the same dimensions is in place. The cassette is manufactured such that it can contain 17 cross-shaped OSLDs lying centrally on the upper side of the cassette plane. The nanodot OSL dosimeters were employed for end-to-end absolute point dosimetry in the RTsafe Prime phantom. For the readout of the irradiated OSLDs the microSTARii® mobile reader was used. The dot readings obtained from the system were converted off-line into dose using the individual calibration factors obtained for each dot, based on exposure to a known dose. The dose response relationship for the OSL detectors in ^{60}Co was investigated for doses ranging from 0.5 to 13 Gy. The calibration factors of the OSLD dosimeters were determined at the Greek Atomic Energy Commission IRCL/EEAE-EIM at a Co-60 beam and the results were calculated in terms of dose (Gy). The OSLDs were irradiated at a depth of 5 cm in a Solid Water HE slab phantom (Sun Nuclear Corporation) for doses ranging from of 0.5 to 13 Gy. Each detector was irradiated a single time to a specified dose and the reading was determined. One detector was used for each dose value. For all subsequent measurements, each detector was read three times following an irradiation and the average of those three readings was taken as the detector signal.

17 OSLDs were placed in the appropriate dosimetry cassette of the Prime phantom. The cassette contains 4 PMMA cylindrical pins in order to facilitate spatial registration of the OSL dose measurements with the exported RTDOSE from the treatment planning system (TPS). The geometric center of the PMMA fiducials is located on the OSLDs plane. Since the position of the sensitive volume of each dosimeter in relation to the CT-identified centers of the pins is well-defined, the corresponding RTDOSE points with which the measurement results are compared are also determined.

For the SRS plan, the dose difference between TPS predicted and OSLD measured doses in the sensitive volume of each dosimeter was calculated and reported as:

$$\frac{D^{TPS} - D^{OSLD}}{D^{OSLD}} \; x \; 100\%$$

The typical uncertainty budget for the OSL calibration, which includes OSL irradiation and reader factors, is presented in the following Table 2. The Type A and Type B columns include the relative standard uncertainties (percentage, for k=1).

The OSL dose is compared to the corresponding point of the RTDOSE, exported from the RT center's TPS in a uniform 1.0 mm resolution grid.

The typical uncertainty budget for the OSL dose measurements, which includes irradiation and OSL and reader factors, is presented in the following table 3. The Type A and Type B columns include the relative standard uncertainties (percentage, for k=1).

Table 2: Uncertainty analysis for the dose distribution measurement on the OSL during the end-to-end procedures using Prime phantom

	Spatial, mm	Type A, %	Type B, %
Calibration factors			
Reference irradiation accuracy (*)	N/A		0.55
Phantom positioning during irradiation (*)	N/A		0.20
Solid water to water dose correction (*)	N/A	0.50	
Dosimeter positioning during irradiation (*)	N/A	0.07	
Dosimeter readout (*)	N/A	0.16	
Individual dosimeter sensitivity (*)	N/A	0.43	
Reader factors			
Stability (*)	N/A	1.00	
Reproducibility (*)	N/A	0.60	
Detector factors			
Dosimeter positioning during irradiation (*)	N/A	0.20	
Dosimeter readout (*)	N/A	0.70	
Energy correction (*)	N/A	0.82	
Fading correction (*)	N/A	0.01	
Registration factors			
OSL plane and positioning (CT, TPS and LINAC)	0.5	N/A	N/A
Combined Type A and Type B standard uncertainties	0.5	1.74	0.59
Combined standard uncertainty, k=1	**0.5**	**1.84**	
Expanded uncertainty, k=2	N/A	**3.67**	

(*) [2–4]

Film dosimetry

The phantom incorporating the film dosimetry cassette, has been described in detail in the publication of Makris et al 2019[1]. The EBT-3 Gafchromic films were employed for end-to-end absolute 2D dosimetry in the RTsafe Prime phantom. Each film piece was handled according to the procedures summarized in Niroomand-Rad et al[5]. The films were scanned on an EPSON V850 Pro flatbed color scanner in transmission mode, with maximum optical density (OD) range and all filters and image enhancement options disabled. All films (calibration and experimental) were labeled and scanned in landscape orientation with respect to the scanning bed, pre- and 24h post-irradiation. RGB positive images are collected at 48-bit RGB with a spatial resolution of 150 dpi (0.169 mm pixel size) and saved as tagged image file format (TIFF) files.

The dose calibration of the film batch was performed in the IRCL/GAEC-EIM at a Co-60 beam. Film pieces of dimensions 4×4 cm^2 were irradiated at a depth of 5 cm in a Solid Water HE slab phantom (Sun Nuclear Corporation) for doses ranging from of 0.10 to 15 Gy.

Each film piece was scanned five times. The obtained images are processed using a custom-made software tool (Graphical User Interface, GUI) developed in MATLAB (MathWorks, Natick, MA). The red, green and blue components of the RGB image are separated. The net Optical Density, netOD, was determined for the red color channel[6]. A polynomial calibration curve was obtained for the red color and was used for conversion of the net optical density values into dose values[7]. Experimental dose maps were also calculated using the single channel method proposed by Devic[7–9].

One film piece 7.5 x 14 cm^2 of the EBT-3 film was placed in the appropriate dosimetry cassette of the Prime phantom. The cassette contains 4 metal pins in order to facilitate film positioning and spatial registration of the film dose distribution with the exported RTDOSE from the TPS. The geometric center of the fiducials is located on the film plane. Matching the CT-identified centers of the fiducials with corresponding positions of the holes in the scanned film image

offers the necessary set of reference points, defining the rigid transformation matrix in order to spatially register film measurements to TPS calculations.

The typical uncertainty budget for the film calibration, which includes film irradiation and scanner factors, is presented in the following Table 4. The Type A and Type B columns include the relative standard uncertainties (percentage, for k=1).

The film dose distribution is compared to the corresponding slice of the RTDOSE, exported from the RT center's TPS in a uniform 0.5 mm resolution grid.

The typical uncertainty budget for the film dose distribution measurement, which includes irradiation and film and scanner factors, is presented in the following table 5. The Type A and Type B columns include the relative standard uncertainties (percentage, for k=1).

To assess whether the QA results meet the pre-defined standards the latest recommendations of the AAPM-RSS Medical Physics Practice Guideline 9.a. for SRS-SBRT[10] are adopted. So, following these recommendations for gamma analysis using global normalization in absolute dose tolerance limits are set as follows:

• Tolerance limits: the γ passing rate should be ≥ 95%, with 5%/1 mm and a 10% low-dose cut-off threshold.

• Action limits: the γ passing rate should be ≥ 90%, with 5%/1 mm and a 10% low-dose cut-off threshold.

Table 3: Uncertainty analysis for the dose distribution measurement on the film during the end-to-end procedures using Prime phantom.

	Spatial, mm	Type A, %	Type B, %	
Calibration factors				
Reference irradiation accuracy	N/A		0.55	
Phantom positioning during irradiation (*)	N/A		0.20	
Solid water to water dose correction (*)	N/A	0.50		
			Dose dependent	
Calibration curve fit parameters (dose dependent)	N/A		2.16	3.17
Scanner factors				
Reproducibility (*)	N/A	0.15		
OD measurement reproducibility	N/A	0.40		
Scanner homogeneity (*)	N/A		0.20	
Registration factors				
OSL plane and positioning (CT, TPS and LINAC)	0.5	N/A	N/A	
Combined Type A and Type B standard uncertainties	0.5	0.66	2.25	3.23
Combined standard uncertainty, k=1	**0.5**	**2.34**	**3.30**	
Expanded uncertainty, k=2	N/A	**4.69**	**6.59**	

(*)[2,11,12]

Gel dosimetry

The phantom incorporating the polymer gel dosimetry insert is similar to the detailed description in the publication of Makris et al 2019[1]. The difference is that instead of the film cassette, the gel-filled cylindrical insert made of glass (2mm wall thickness) is in place. The polymer gel formulation characterized in Saenz et al 2021[13] is used. After irradiation, the phantom is left for 24h at room temperature (20-22^{o}C) to allow for polymerization growth and stabilization. For the MR dose read-out, the Prime phantom incorporating the irradiated gel cylinder is scanned 24 hours post-irradiation at the RTsafe reference MR scanner (model SIEMENS MAGNETOM Sonata/Vision) using a birdcage head coil. MR acquisition is performed with a 2D multi-echo HASTE sequence, which consists of 4 echoes with the first one at 36 ms and echo time intervals of 400 ms. In order to minimize MR-related geometric distortion, the highest bandwidth value is selected (780 Hz/pixel)[14] for the MRI read-out (the distortion correction algorithm provided by Siemens to minimize the MR distortions due to gradient non-linearities is also enabled). However, this comes at the expense of reduced SNR, so the number of averages (number of acquisitions) is set to 20 in order to increase SNR. The scan length on the superior – inferior direction (i.e., z-axis) extends to cover the entire phantom volume. The MR scanning time was approximately 30 min for a voxel size of 1.37 × 1.37 × 2 mm^3. A T2 map is calculated for each slice and the resulting T2 image series are imported in the Elekta Monaco 5.51.01 (Elekta, Stockholm, Sweden) TPS and co-registered with the treatment planning CT images. The fused T2 images are then exported from the TPS in the CT resolution allowing the detailed 3D qualitative comparison between TPS-calculations and corresponding polymer gel-derived measurements. Calculation of the corresponding R2 (i.e. R2=1/T2) relaxation rate maps in 3D is performed using in-house MATLAB routines which have been verified in the literature[14,15]. The dose response, measured as R2 relaxation rate, exhibits a linear dependence on the applied dose[16]. Geometry offset calculations are allowed by comparing the gel-derived and TPS 3D dose distributions in terms of relative dose. In detail, spatial offsets are measured independently for each target by comparing in 3D the center-of-mass (CoM) of

the polymerized area with the center-of-mass of the planned high-dose area. The center of mass of each distribution is calculated by averaging the center of mass coordinates of the consecutive dose distributions derived by applying a range of dose thresholds (50%-70% relative dose levels of the prescription dose with a step of 5%), taking into account the dose gradient of each target and the spatial resolution of the MR images used for gel readout[17]. To assess the total spatial offset of the planned dose distribution and the corresponding gel-measured dose distribution for each target, the geometric distance between the center of masses is calculated.

The specific end-to-end procedure also takes into account the uncertainty associated with the spatial registration of MR to CT images. Polymer gel measured spatial offsets incorporate an uncertainty component derived from the spatial distortions that are inherent to the MR images used for the gel readout[18]. However, MR spatial distortions within the cylindrical volume of the polymer gel insert (when centered at the scanner's isocenter) for the MR sequence used herein are expected to affect the total offset results by no more than the statistical uncertainty of the method.

References

1. Makris DN, Pappas EP, Zoros E, et al. Characterization of a novel 3D printed patient specific phantom for quality assurance in cranial stereotactic radiosurgery applications. *Phys Med Biol*. 2019;64(10). doi:10.1088/1361-6560/ab1758
2. Wesolowska PE, Cole A, Santos T, Bokulic T, Kazantsev P, Izewska J. Characterization of three solid state dosimetry systems for use in high energy photon dosimetry audits in radiotherapy. *Radiat Meas*. 2017;106:556-562. doi:10.1016/j.radmeas.2017.04.017
3. Viamonte A, Da Rosa LAR, Buckley LA, Cherpak A, Cygler JE. Radiotherapy dosimetry using a commercial OSL system. *Med Phys*. 2008;35(4):1261-1266. doi:10.1118/1.2841940
4. Yukihara EG, Yoshimura EM, Lindstrom TD, Ahmad S, Taylor KK, Mardirossian G. High-precision dosimetry for radiotherapy using the optically stimulated luminescence technique and thin Al2O3:C dosimeters. *Phys Med Biol*. 2005;50(23):5619-5628. doi:10.1088/0031-9155/50/23/014
5. Niroomand-Rad A, Chiu-Tsao ST, Grams MP, et al. Report of AAPM Task Group 235 Radiochromic Film Dosimetry: An Update to TG-55. *Med Phys*. 2020;47(12):5986-6025. doi:10.1002/mp.14497
6. Méndez I. Model selection for radiochromic film dosimetry. *Phys Med Biol*. 2015;60:4089-4104.
7. Devic S, Seuntjens J, Sham E, et al. Precise radiochromic film dosimetry using a flat-bed document scanner. *Med Phys*. 2005;32(7Part1):2245-2253. doi:10.1118/1.1929253
8. Devic S, Tomic N, Lewis D. Reference radiochromic film dosimetry: Review of technical aspects. *Phys Medica*. 2016;32(4):541-556. doi:10.1016/j.ejmp.2016.02.008
9. Devic S, Seuntjens J, Hegyi G, et al. Dosimetric properties of improved GafChromic films for seven different digitizers. *Med Phys*. 2004;31(9):2392-2401. doi:10.1118/1.1776691
10. Halvorsen PH, Cirino E, Das IJ, et al. AAPM-RSS Medical Physics Practice Guideline 9.a. for SRS-SBRT. *J Appl Clin Med Phys*. 2017;18(5):10-21. doi:10.1002/acm2.12146
11. Mathot M, Sobczak S, Hoornaert MT. Gafchromic film dosimetry: Four years experience using FilmQA Pro software and Epson flatbed scanners. *Phys Medica*. 2014;30(8):871-877. doi:10.1016/j.ejmp.2014.06.043
12. Aldelaijan S, Mohammed H, Tomic N, et al. Radiochromic film dosimetry of HDR 192Ir source radiation fields. *Med Phys*. 2011;38(11):6074-6083. doi:10.1118/1.3651482
13. Robustness of single-isocenter multiple-metastasis stereotactic radiosurgery end-to-end testing across institutions - PubMed. Accessed May 24, 2021. https://pubmed.ncbi.nlm.nih.gov/33898086/
14. Hillbrand M, Landry G, Ebert S, et al. Gel dosimetry for three dimensional proton range measurements in anthropomorphic geometries. *Z Med Phys*. 2019;29(2):162-172. doi:10.1016/j.zemedi.2018.08.002
15. Saenz DL, Li Y, Rasmussen K, Stathakis S, Pappas E, Papanikolaou N. Dosimetric and localization accuracy of Elekta high definition dynamic radiosurgery. *Phys Medica*. 2018;54(August):146-151. doi:10.1016/j.ejmp.2018.10.003
16. Pappas E, Maris T, Angelopoulos A, et al. A new polymer gel for magnetic resonance imaging (MRI) radiation dosimetry. *Phys Med Biol*. 1999;44(10):2677-2684. doi:10.1088/0031-9155/44/10/320
17. Pantelis E, Moutsatsos A, Antypas C, et al. On the total system error of a robotic radiosurgery system: Phantom measurements, clinical evaluation and long-term analysis. *Phys Med Biol*. 2018;63(16). doi:10.1088/1361-6560/aad516
18. Moutsatsos A, Karaiskos P, Petrokokkinos L, et al. On the use of polymer gels for assessing the total geometrical accuracy in clinical Gamma Knife radiosurgery applications. *J Phys Conf Ser*. 2010;250:292-296. doi:10.1088/1742-6596/250/1/012060